

PrivateSNN: Fully Privacy-Preserving Spiking Neural Networks

Youngeun Kim
Yale University

youngeun.kim@yale.edu

Yeshwanth Venkatesha
Yale University

yeshwanth.venkatesha@yale.edu

Priyadarshini Panda
Yale University

priya.panda@yale.edu

Abstract

How can we bring both privacy and energy-efficiency to a neural system on edge devices? In this paper, we propose PrivateSNN, which aims to build low-power Spiking Neural Networks (SNNs) from a pre-trained ANN model without leaking sensitive information contained in a dataset. Here, we tackle two types of leakage problems: 1) Data leakage caused when the networks access real training data during an ANN-SNN conversion process. 2) Class leakage is the concept of leakage caused when class-related features can be reconstructed from network parameters. In order to address the data leakage issue, we generate synthetic images from the pre-trained ANNs and convert ANNs to SNNs using generated images. However, converted SNNs are still vulnerable with respect to the class leakage since the weight parameters have the same (or scaled) value with respect to ANN parameters. Therefore, we encrypt SNN weights by training SNNs with a temporal spike-based learning rule. Updating weight parameters with temporal data makes networks difficult to be interpreted in the spatial domain. We observe that the encrypted PrivateSNN can be implemented not only without the huge performance drop (less than $\sim 5\%$) but also with significant energy-efficiency gain (about $\times 60$ compared to the standard ANN). We conduct extensive experiments on various datasets including CIFAR10, CIFAR100, and TinyImageNet, highlighting the importance of privacy-preserving SNN training.

1. Introduction

Neuromorphic computing has gained considerable attention as an energy-efficient alternative to conventional Artificial Neural Networks (ANNs) [18, 46, 13, 12]. Especially, Spiking Neural Networks (SNNs) process binary spikes through time like a human brain, resulting in 1-2 order of magnitude energy efficiency over ANNs on emerging neuromorphic hardware [42, 11, 1, 4]. Due to the energy advantages and neuroscientific interest, SNNs have made great strides on various applications such as image recognition [31, 26, 6], visualization [27], optimization [8, 9], and

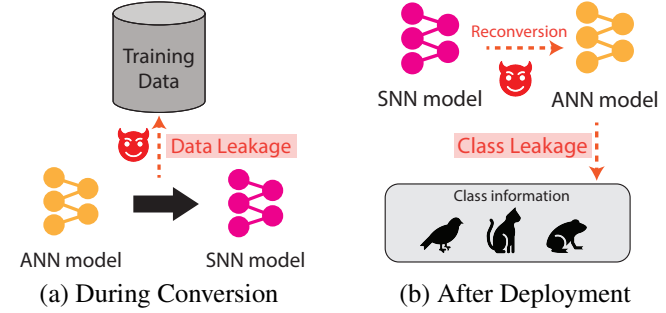


Figure 1. Illustration of data leakage and class leakage problems. (a) The data leakage problem is likely to happen when an ANN model accesses real data during conversion process. (b) The malicious attacker can obtain class information by reconverting the SNN model to the ANN model.

object detection [24]. Therefore, SNNs have a huge potential to be exploited on real-world edge devices.

Consequently, various SNN training techniques have been proposed in order to build SNNs as a future Artificial Intelligence (AI) system. Spike-timing-dependent plasticity (STDP) based on the neuroscience studies of mammalian brain development reinforces or penalizes the weight connection based on their spike history [2, 19, 3, 49]. Surrogate gradient learning techniques circumvent the non-differentiable problem of a Leak-Integrate-and-Fire (LIF) neuron by defining an approximated backward gradient function [31, 30, 39]. ANN-SNN conversion techniques convert pre-trained ANNs to SNNs using weight or threshold balancing in order to replace ReLU activation with LIF activation. [44, 16, 7, 43]. Compared to the other methods, ANN-SNN conversion is well-established and achieves high performance on complex datasets. Therefore, ANN-SNN conversion can be a prospective candidate for neuromorphic systems on various applications.

Existing conversion algorithms are based on the assumption that the model can access the entire training data. Specifically, they pass the training samples through the networks and use the maximum activation value for calculating layer-wise threshold (or weight). However, this may not always be feasible. After the ANN model is transferred on

a neuromorphic device, there is the possibility that training data might be corrupted or lost [33]. Also, training datasets like ImageNet are too large to transfer from server to edge devices [38]. Furthermore, enterprises would not allow proprietary information to be shared publicly with rival companies and individuals. Most importantly, the training set may contain sensitive information such as biometrics. Overall, these concerns about privacy motivates a line of research on privacy-preserving algorithms [29, 25, 38, 32, 17, 34]. We refer this problem as **data leakage** (Fig. 1(a)).

In addition, we tackle a **class leakage** problem after deployment (*i.e.*, inference), as shown in Fig. 1(b). It is a well known fact that one can obtain a representative class image from model parameters by using simple gradient back-propagation [37, 50]. From a security perspective, revealing class information can induce a critical situation in a neural system. A malicious attacker can find a blind spot of neural systems, and use these unrecognizable classes/pattern to disguise a system in real-world. Also, class information can be exploited to generate a strong adversarial attack [14]. For instance, Mopuri *et al.* [37] use synthetic class representation to generate Universal Adversarial Perturbations (UAP). Therefore, to build a secured neural system on edge devices, the class leakage problem should be addressed rigorously. It is worth mentioning that the class leakage problem is similar to the model inversion attack [10, 52] in that it reconstructs input representation from the pre-trained model. But we aim to generate conceptual class images whereas model inversion attack tries to recover sophisticated input representation. Also, the class leakage problem is different from the gradient leakage problem [54, 53] that aims to recover original image data from gradients on a federated learning scenario.

In this paper, we propose *PrivateSNN*, a new ANN-SNN conversion paradigm that addresses both data leakage and class leakage problems. To address the data leakage issue, we generate synthetic data samples from the pre-trained ANN model and conduct ANN-SNN conversion using generated data. Unfortunately, even though the data leakage problem is addressed, class leakage is still problematic since the attacker can easily recover class information from weight parameters. Therefore, we encrypt the weight parameters with the temporal spike-based learning rule. We encode a synthetic image into spike trains and finetune converted SNNs on temporal data. Also, considering the resource-constrained device where SNNs are likely to be applied, SNNs might be limited to use a small number of training samples due to computational cost for training. To preserve the performance with a small dataset, we distill the knowledge from ANN to regularize SNN training. As a result, encrypted SNNs with temporal information open a new pathway for a fully privacy-preserving and energy-efficient neuromorphic system.

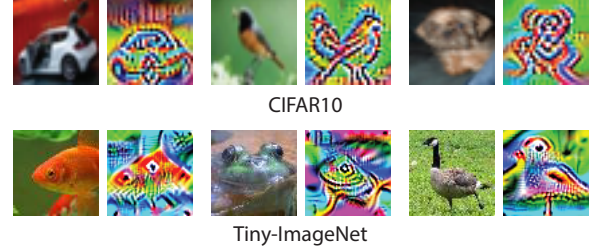


Figure 2. Examples of class leakage. We use VGG16 trained on CIFAR10 and Tiny-ImageNet. We visualize pair of images (left: real image, right: generated image) for each sample. For CIFAR10, we visualize automobile, bird, and dog. For Tiny-ImageNet, we visualize goldfish, bullfrog, and goose.

In summary, our key contributions are as follows: (i) So far, in SNN literature, there is no discussion about the privacy issue of ANN-SNN conversion. For the first time, we tackle the privacy issues of a neuromorphic system that has a huge potential to be deployed on edge devices. (ii) We define two leakage problems (*i.e.*, data leakage and class leakage) that are likely to happen during the conversion process. Further, we present how to generate class leakage from the SNN model. (iii) We propose *PrivateSNN* which successfully converts ANNs to SNNs without exposing sensitive information of data. We encrypt the weight parameters of SNNs with the temporal learning rule. Also, distillation from the ANN model to SNNs enables stable encryption training with a small number of samples. (iv) We conduct extensive experiments on various datasets including CIFAR10, CIFAR100, and TinyImageNet. The results show that the proposed *PrivateSNN* yields both energy-efficiency and privacy-preserving advantages.

2. The Vulnerability of ANN-SNN Conversion

In this section, we present the ANN-SNN conversion algorithm and show two possible leakage problems.

2.1. ANN-SNN Conversion

Our model is based on Leaky-Integrate-and-Fire (LIF) neuron. The internal state of an LIF neuron is represented by a membrane potential U_m . As time goes on, the membrane potential decays with time constant τ_m . Given an input signal $I(t)$ and an input register R at time t , the differential equation of the LIF neuron can be formulated as:

$$\tau_m \frac{dU_m}{dt} = -U_m + RI(t). \quad (1)$$

This continuous dynamic equation is converted into a discrete equation for digital simulation. More concretely, we formulate the membrane potential u_i^t of a single neuron i as:

$$u_i^t = \lambda u_i^{t-1} + \sum_j w_{ij} o_j^t, \quad (2)$$

Algorithm 1 ANN-SNN Conversion [44]

Input: input set (X); label set (Y); max timestep (T); pre-trained ANN model (ANN); SNN model (SNN); total layer number (L)
Output: updated SNN network with threshold balancing

```

1:  $SNN.weights \leftarrow ANN.weights$             $\triangleright$  Copy weights
2:  $SNN.th \leftarrow 0$                            $\triangleright$  Initialize threshold voltage
3: for  $l \leftarrow 1$  to  $L - 1$  do
4:   for  $t \leftarrow 1$  to  $T$  do
5:      $O^t \leftarrow \text{PoissonGenerator}(X)$ 
6:     for  $l_{current} \leftarrow 1$  to  $l$  do
7:       if  $l_{current} < l$  then
8:          $(O_l^t, U_l^t) \leftarrow (U_l^{t-1}, W_l, O_{l-1}^t)$ 
9:       else
10:         $SNN_l.th \leftarrow \max(SNN_l.th, W_l O_{l-1}^t)$ 
11:       end if
12:     end for
13:   end for
14: end for

```

where, λ is a leak factor, w_{ij} is a the weight of the connection between pre-synaptic neuron j and post-synaptic neuron i . If the membrane potential u_i^t exceeds a firing threshold θ , the neuron i generate spikes o_i^t , which can be formulated as:

$$o_i^t = \begin{cases} 1, & \text{if } u_i^t > \theta, \\ 0 & \text{otherwise.} \end{cases} \quad (3)$$

After the neuron fires, we perform a soft reset, where the membrane potential value u_i^t is lowered by the threshold θ .

We use the method described by [44] for implementing the ANN-SNN conversion. They normalize the weights or the firing threshold (θ in Eq. 3) to take into account the actual SNN operation in the conversion process. The overall algorithm for the conversion method is shown in Algorithm 1. First, we copy the weight parameters of a pre-trained ANN to an SNN. Then, for every layer, we compute the maximum activation across all time-steps and set the firing threshold to the maximum activation value. The conversion process starts from the first layer and sequentially goes through deeper layers. Note that we do not use batch normalization [23] since all input spikes have zero mean values. Also, following the previous works [16, 44, 7], we use Dropout [47] for both ANNs and SNNs.

2.2. Two Types of Leakage Problems

Data Leakage from Public Datasets: Algorithm 1 shows that the entire training data is required to convert ANNs to SNNs. However, due to the privacy issue of a dataset, we might not be able to access the training samples. This issue is highly important for a secure AI system, and therefore has been addressed in various applications such as quantization, model compression, distillation, and domain adaptation [29, 25, 38, 32, 17, 34]. Therefore there is a need to develop a data-free conversion algorithm in the

Algorithm 2 Class representative image generation

Input: target class (c); max iteration (N); blurring frequency (f_{blur}); learning rate (η)
Output: class representative image x

```

1:  $x \leftarrow U(0, 1)$             $\triangleright$  Initialize input as uniform random distribution
2: for  $n \leftarrow 1$  to  $N$  do
3:   if  $n \% f_{blur} == 0$  then
4:      $x \leftarrow \text{GaussianBlur}(x)$ 
5:   end if
6:    $y \leftarrow \text{network}(x)$             $\triangleright$  compute pre-softmax output  $y$ 
7:    $x \leftarrow x + \eta \frac{\partial y_c}{\partial x}$ 
8: end for

```

neuromorphic domain.

Class Leakage from Reverting SNNs to ANNs: In addition to the data leakage problem, class information, *e.g.*, pattern and shape of the object, also can be targeted by the attacker. Algorithm 2 presents a simple way to obtain class representative information from an ANN model. First, we initialize the input tensor with uniform random distribution. After that, we use an iterative optimization strategy where input noise is updated to maximize the pre-softmax logit y_c of target class c . For every blur period f_{blur} , we smooth the image with Gaussian Blur kernel since gradient at input layer has a high frequency [50]. Fig. 2 shows examples of class representative images generated from a pre-trained model.

However, this technique is based on the assumption that we can compute the exact gradient for all layers. It is difficult to compute gradient value of SNNs due to the non-differentiable nature of LIF neuron (Eq. 2 and Eq. 3). Therefore, in order to generate proper class representation, the attacker should reconvert SNNs to ANNs. The reconversion process depends on the type of conversion technique; weight scaling or threshold scaling. There are several conversion algorithms [43, 7] that scales weight parameters of each layer. In such cases, the attacker cannot directly recover original ANN weights. However, each layer is scaled by a constant value, therefore the original ANN weights might be recovered by searching several combinations of layer-wise scaling factors. Also, recent state-of-the-art conversion algorithms [44, 16, 15] change the thresholds while maintaining the weight parameters (*i.e.*, threshold scaling) to obtain high performance. Therefore, in our experiments, we use threshold scaling for ANN-SNN conversion and then, explore the class leakage issues. In this case, the original ANN can be reconverted by simply changing LIF neuron to ReLU neuron. With the reconverted ANN, the attacker can simply reconstruct class representation by back-propagation as shown in Algorithm 2. Overall, a non-linear weight encryption technique is required to make SNNs robust to class leakage.

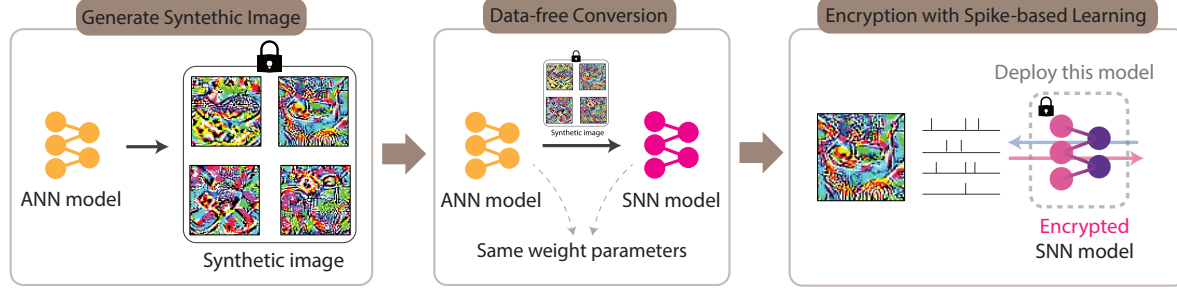


Figure 3. Overview of the proposed *PrivateSNN*. We first generate synthetic images based on underlying data distribution from a pre-trained model. Then, based on the generated samples, we convert the ANN to a SNN model. Finally, we encode synthetic images to spike signal, and train the converted SNN. The weight parameter is encrypted with temporal information. We deploy the final encrypted SNN model for inference.

3. Methodology

This section presents a detailed methodology for *PrivateSNN*. We first propose a data-free conversion method from a pre-trained model. Then, we describe how a temporal spike-based learning rule can encrypt weight parameters in SNNs.

3.1. Data-Free Conversion

Data Generation from a Pre-trained Model: Without accessing real data, we generate synthetic images from a pre-trained model. Conversion performance relies on the maximum activation value of features, therefore synthetic images have to carefully reflect underlying data distribution from a pre-trained ANN model. Nayak *et al.* [38] take into account the relationship between classes in order to generate data, resulting in better performance on a distillation task. Following this pioneering work, we generate synthetic images based on class relationships from the weights of the last fully-connected layer. Specifically, we can define a weight vector w_c between the penultimate layer and the class logit c in the last layer. Then, we calculate the class similarity score between class i and j :

$$s_{ij} = \frac{w_i^T w_j}{\|w_i\|_2^2 \|w_j\|_2^2}. \quad (4)$$

Then, we sample a soft label based on Dirichlet distribution where a concentration parameter α_c is a class similarity vector of class c . For each class c , the class similarity vector consists of class similarity between class c and other classes. For example, for class 1 of CIFAR10 dataset, the concentration parameter is $\alpha_1 = [s_{10}, s_{11}, s_{12}, \dots, s_{19}]$. For a sampled soft label from Dirichlet distribution, we optimize input x initialized with uniform random distribution. We collect the same number of samples for each class and exploit this synthetic dataset for conversion.

ANN-SNN Conversion with synthetic images: By generating synthetic images, we do not have to access the original dataset. Instead, we find the threshold of each layer from

Algorithm 3 PrivateSNN Approach

Input: total class set (C); the number of samples per class (N); pre-trained ANN model (ANN); SNN model (SNN); spike time-step (T); distillation temperature (τ);

Output: encrypted SNN model

```

1: [Step1] Data-free conversion
2:  $D \leftarrow \emptyset$  ▷ Initialize synthetic dataset  $D$ 
3: for  $c \leftarrow 1$  to  $C$  do
4:    $\alpha_c \leftarrow ANN.fc.weight$  ▷ Compute class similarity
5:   for  $n \leftarrow 1$  to  $N$  do
6:      $y \sim Dir(\alpha_c)$  ▷ Sample soft label from Dirichlet
7:      $x \leftarrow U(0, 1)$  ▷ Initialize input
8:     Find  $x$  that minimizes  $L_{CE}(ANN(x), y)$ 
9:      $D \leftarrow D \cup \{x\}$ 
10:  end for
11: end for
12: Do ANN-SNN conversion (Algorithm 1) with synthetic dataset  $D$ 
13: [Step2] Encryption with spike-based learning
14: for  $i \leftarrow 1$  to  $max\_iter$  do
15:   fetch a mini batch  $X \subset D$ 
16:   for  $t \leftarrow 1$  to  $T$  do
17:      $O \leftarrow PoissonGenerator(X)$ 
18:     for  $l \leftarrow 1$  to  $L - 1$  do
19:        $(O_l^t, U_l^t) \leftarrow (\lambda, U_l^{t-1}, (W_l, O_{l-1}^t))$ 
20:     end for
21:      $U_L^t \leftarrow (U_L^{t-1}, (W_l, O_{L-1}^t))$  ▷ Final layer
22:   end for
23:    $L_{CE} \leftarrow (U_L^T, Y)$ 
24:    $L_{KD} \leftarrow (ANN(X, \tau), SNN(X, \tau))$ 
25:   Do back-propagation and weight update
26: end for

```

the maximum activation of synthetic images (Algorithm 1). Interestingly, we observe that converted SNNs with synthetic images almost recover the performance of the original ANN. This means that conversion process is feasible with inherent data distribution from a trained model. However, SNNs are still vulnerable to class leakage. If the attacker transmits the weight of SNNs to their computational plat-

form, they can easily recover the original ANN by simply changing the LIF neuron to ReLU. Therefore, we encrypt a model using the temporal spike-based learning rule (will be described in the next subsection). Here, we use a relatively small number of time-steps (e.g., $100 \sim 200$) for conversion. This is because short time-steps reduces training time and memory for post-conversion training. Also, short latency can bring more energy efficiency at inference. We observe that encryption training recovers the performance loss caused by using a small number of time-steps for conversion.

3.2. Encryption with Spike-based Learning Rule

The key idea here is that training SNNs with temporal data representation makes networks difficult to be interpreted in the spatial domain.

Encoding static images with rate coding: In order to map static images to temporal signals, we use rate coding (or Poisson coding). Given the time window, rate coding generates spikes where the number of spikes is proportional to the pixel intensity. For time-step t , we generate a random number for each pixel (i, j) with normal distribution ranging between $[I_{min}, I_{max}]$, where I_{min}, I_{max} correspond to the minimum and maximum possible pixel intensity. After that, for each pixel location, we compare the pixel intensity with the generated random number. If the random number is greater than the pixel intensity, the Poisson spike generator outputs a spike with amplitude 1. Otherwise, the Poisson spike generator does not yield any spikes. Overall, rate coding enables static images to span on the temporal axis without huge information loss.

Training SNNs with spike-based learning rule: Given input spikes, we train converted SNNs based on gradient optimization. Intermediate LIF neurons accumulate pre-synaptic spikes and generate output spikes (Eq. 2 and Eq. 3). Spike information is passed through all layers and stacked at the output layer (*i.e.*, prediction layer) which does not generate any spikes. This enables temporal spikes to be represented as probability distribution after the softmax function. From the accumulated membrane potential, we can define the cross-entropy loss for SNNs as:

$$L_{CE} = - \sum_i y_i \log \left(\frac{e^{u_i^T}}{\sum_{k=1}^C e^{u_k^T}} \right), \quad (5)$$

where, y and T stand for the ground-truth label and the total number of time-steps, respectively.

One important thing we have to consider is the computational cost for post-conversion training. This is crucial to a limited-resource environment such as a mobile device with battery constraints. Also, SNNs require multiple feed-forward steps per one image, which has a more energy-consuming training process compared to ANN. In order to

reduce energy for training, we can reduce the number of synthetic training samples. However, with a small number of training samples, the networks easily overfit to small training set, resulting in performance degradation. To address this issue, we distill knowledge from ANNs to SNNs. Yuan *et al.* [51] recently discovered the connection between knowledge distillation and label smoothing, which supports distillation improves the generalization power of the model. Thus, it is intuitive that if we use knowledge distillation then the model is likely to show a better generalization to small data samples. Therefore, the total loss function becomes the combination of cross-entropy loss and distillation loss:

$$L = (1 - m)L_{CE} + mL_{KD}(A(X, \tau), S(X, \tau)). \quad (6)$$

Here, $A(\cdot)$ and $S(\cdot)$ represent ANN and SNN models, respectively. Also, τ denotes distillation temperature, and m is the balancing coefficient between two losses. Note that L_{KD} is knowledge distillation loss [21]. Surprisingly, we found that SNNs (on CIFAR10) with distillation loss almost maintain its performance even with only 100 synthetic training samples (0.2% of the total number of samples in the original CIFAR10 training set).

Based on Eq. 6, we compute the gradients of each layer l . Here, we use spatio-temporal back-propagation (STBP), which accumulates the gradients over all time-steps [48, 39]. We can formulate the gradients at the layer l by chain rule as:

$$\frac{\partial L}{\partial W_l} = \begin{cases} \sum_t \left(\frac{\partial L}{\partial O_l^t} \frac{\partial O_l^t}{\partial U_l^t} + \frac{\partial L}{\partial U_l^{t+1}} \frac{\partial U_l^{t+1}}{\partial U_l^t} \right) \frac{\partial U_l^t}{\partial W_l}, & \text{if } l : \text{hidden} \\ \frac{\partial L}{\partial U_l^T} \frac{\partial U_l^T}{\partial W_l}. & \text{if } l : \text{output} \end{cases} \quad (7)$$

Here, O_l^t and U_l^t are output spikes and membrane potential at time-step t for layer l , respectively. For the output layer, we get the derivative of the loss L with respect to the membrane potential u_l^T at final time-step T :

$$\frac{\partial L}{\partial u_l^T} = \frac{e^{u_l^T}}{\sum_{k=1}^C e^{u_k^T}} - y_i. \quad (8)$$

This derivative function is continuous and differentiable for all possible membrane potential values. On the other hand, LIF neurons in hidden layers generate spike output only if the membrane potential u_i^t exceeds the firing threshold, leading to non-differentiability. To deal with this problem, we introduce an approximate gradient:

$$\frac{\partial o_i^t}{\partial u_i^t} = \max\{0, 1 - |\frac{u_i^t - \theta}{\theta}| \}, \quad (9)$$

Overall, we update the network parameters at the layer l based on the gradient value (Eq. 7) as $W_l = W_l - \eta \Delta W_l$.

Training SNNs after conversion is not a new technique. Rathi *et al.* [41] proposed hybrid training by combining

conversion and gradient-based learning. However, their objective was to improve the model performance in a low time-step regime with a real image dataset. In contrast to their work, our training aims to encrypt SNNs without accessing the original dataset. Moreover, we present distillation from ANN to SNN, which enables encryption training with only a small number of training samples.

4. Attack Scenarios for Class Leakage

In this section, we present two possible attack scenarios on class leakage. Since we do not access the original training data, the data leakage problem is addressed. Therefore, here we only discuss the class leakage problem.

Attack scenario 1 (Reconverting SNN to ANN): As discussed in Section 2.2, the attacker might copy the weights of SNN and recover the original ANN. By using the re-converted ANN, the attacker optimizes the input noise based on Algorithm 2. Without post-conversion training, the attacker simply reconstructs class representation by backpropagation. However, if we use spike-based training, the weight of ANN is fully encrypted in the spatial domain.

Attack scenario 2 (Directly generate class representation from SNN): The attacker might directly backpropagate gradients in SNN architecture and reconstruct class representation. Thus, this is the SNN version of Algorithm 2. The technical problem here is that LIF neurons and a Poisson spike generation process are non-differentiable. To address this issue, we use approximated gradient functions (Eq. 9) for LIF neurons. Also, in order to convert the gradient in the temporal domain to the spatial domain, we accumulate gradient at the first convolution layer. After that, we deconvolve the accumulated gradients with weights of the first layer. These deconvolved gradients have a similar value with original gradients of images before the Poisson spike generator, which has been validated in the previous work [45]. Thus, we can get a gradient δx converted into spatial domain, and the input noise is updated with gradient δx scaled by ζ . Algorithm 4 illustrates the overall optimization process. However, this attack does not show meaningful features due to the discrepancy between real gradients and approximated gradients. This supports that SNN model itself is robust to gradient-based security attacks. We show the qualitative results in the Fig. 6.

5. Experiments

5.1. Experimental Setting

We evaluate our *PrivateSNN* on three public datasets (*i.e.*, CIFAR-10, CIFAR-100, Tiny-ImageNet). **CIFAR-10** [28] consists of 60,000 images (50,000 for training / 10,000 for testing) with 10 categories. All images are RGB color images whose size are 32×32 . **CIFAR-100** has the same configuration as CIFAR-10, except it contains images from

Algorithm 4 Directly generate class representation from SNNs (Attack scenario 2)

Input: target class (c); max iteration (N); scaling factor (ζ); SNN model (SNN); spike time-step (T)

Output: class representative image x

```

1:  $x \leftarrow U(0, 1)$                                  $\triangleright$  Initialize input
2:  $W_1 \leftarrow SNN.conv1.weight$                    $\triangleright$  First convolution weight
3:  $G = 0$                                           $\triangleright$  Accumulated gradient at the first conv layer
4: for  $n \leftarrow 1$  to  $N$  do
5:   for  $t \leftarrow 1$  to  $T$  do
6:      $y \leftarrow SNN(x_t)$ 
7:      $G+ = \frac{1}{T} \frac{\partial y_c}{\partial x_{conv1}}$    $\triangleright$  Accumulate gradients in layer 1
8:   end for
9:    $\delta x \leftarrow Deconvolution(W_1, G)$            $\triangleright$  Deconvolution
10:   $x \leftarrow x + \zeta \delta x$ 
11: end for

```

100 categories. **Tiny-ImageNet** is the modified subset of the original ImageNet dataset. Here, there are 200 different classes of ImageNet dataset [5], with 100,000 training and 10,000 validation images. The resolution of the images is 64×64 pixels.

Our implementation is based on Pytorch [40]. In conversion process, we apply threshold scaling technique (*i.e.*, multiplying constant to thresholds of all layers, we set scaling factor to 0.7) proposed in [16]. We use 1000, 1000, and 2000 synthetic samples for converting ANNs trained on CIFAR10, CIFAR100, and TinyImageNet, respectively. For post-conversion training, we use Adam with base learning rate 1e-4. Here, we use 5000, 10000, 10000 synthetic samples for training SNNs on CIFAR10, CIFAR100, and TinyImageNet, respectively. We use step-wise learning rate scheduling with a decay factor 10 at 50% and 70% of the total number of epochs. We set the total number of epochs to 20 for all datasets. For distillation, we set m and τ to 0.7 and 20 in Eq. 6, respectively. For class representation, we set f_{bulr} and η in Algorithm 2 to 4 and 6, respectively. For attack scenario 2 in Algorithm 4, we set ζ to 0.01. Note that our objective is to compare *PrivateSNN* with conventional ANN-SNN conversion.

5.2. Conversion Performance

Surprisingly, we find that *PrivateSNN* encrypts the networks without significant performance loss. Table 1 shows the performance of reference ANN (*i.e.*, VGG16) and previous methods which uses real data. It is worth noting that converted SNNs cannot achieve higher performance than the ANN (*i.e.*, the accuracy of ANN is the upper bound). Here, we use the conversion method proposed in [44] as a representative state-of-the-art conversion method, achieving a similar performance with the reference ANN. The results show that our *PrivateSNN* can be designed without a huge performance drop across all datasets. This implies that

Table 1. Classification Accuracy (%) on CIFAR10, CIFAR100, and TinyImageNet. We report the accuracy of VGG16 architecture in our experiments as a reference. Also, we reimplement [44] and use this work as a baseline.

Method	Require training data?	Dataset	Acc (%)
VGG16 [46]	-	CIFAR10	91.6
Sengupta <i>et al.</i> [44]	Yes	CIFAR10	91.5
PrivateSNN (ours)	No	CIFAR10	91.2
VGG16 [46]	-	CIFAR100	64.3
Sengupta <i>et al.</i> [44]	Yes	CIFAR100	62.7
PrivateSNN (ours)	No	CIFAR100	62.3
VGG16 [46]	-	TinyImageNet	51.9
Sengupta <i>et al.</i> [44]	Yes	TinyImageNet	50.6
PrivateSNN (ours)	No	TinyImageNet	46.2

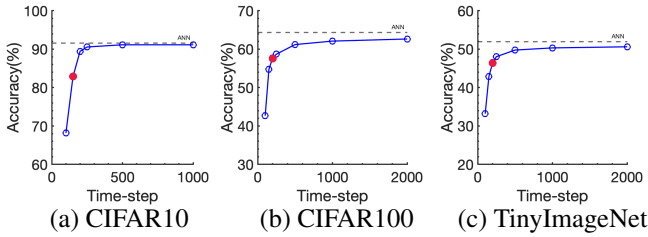


Figure 4. Conversion performance with synthetic images before encryption training. We use small number of time-steps for efficient post-conversion training (marked by red dot).

Table 2. Performance comparison between after conversion and after post encryption training.

Dataset	#Time-step	After Conversion	After Encryption
CIFAR10	100	68.2	91.2
CIFAR100	150	54.7	62.3
TinyImageNet	150	42.9	46.2

synthetic samples generated from the ANN model contain enough information for a successful conversion and post-training processes.

In Fig. 4, we measure the conversion performance with respect to the number of time-steps in the conversion process (Parameter T in Algorithm 1). The results show that the SNN model can recover the original ANN performance with a high number of time-steps. But for post encryption training, we use a small number of time-steps instead of using long time-steps. Specifically, we use time-step 1000, 2000, 2000 for the reference conversion technique [44] on CIFAR10, CIFAR100, and TinyImageNet, respectively. On the other hand, *PrivateSNN* is trained with time-step 100, 150, and 150 for CIFAR10, CIFAR100, and TinyImageNet, respectively (marked by red dot in Fig. 4). This is because a short time-step brings more energy-efficiency during both training and inference. Also, we observe that encryption training with distillation recovers the accuracy even though SNNs are converted in a low time-step regime (Table 2).

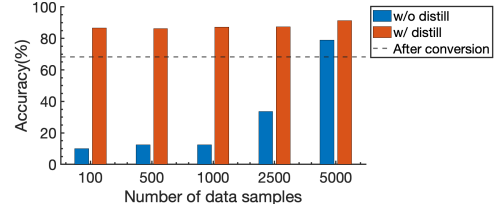


Figure 5. Performance with respect to the number of training samples using encryption training. We use VGG16 trained on CIFAR10.

Table 3. FIDs between test set and generated images from reconverted ANN (**Attack scenario 1**) and backward gradients on SNNs (**Attack scenario 2**).

Method (Dataset: CIFAR10)	w/o Encryption	w/ Encryption
Attack scenario 1	354.8	448.2
Attack scenario 2	447.9	422.4

5.3. Effect of Distillation in Encryption Training

After converting ANNs to SNNs, we train the networks with synthetic images. In order to figure out how many samples are required for post training, we show the performance with respect to the number of synthetic samples in Fig. 5. Note, data-free conversion at 100 time-steps achieves 68.2 % accuracy (back dotted line in the figure). The results show that encryption training (without distillation) degrades the performance significantly with a small number of samples. Interestingly, with distillation, the network almost preserves the performance. Thus, distillation is an effective regularization method for spike-based learning with a small number of synthetic images, which is essential for deploying SNNs on mobile devices.

5.4. Robustness on Class Leakage Problem

In this work, we presented two possible attack scenarios on class leakage (*i.e.*, attack scenario 1 and attack scenario 2) in Section 4. To validate the robustness of *PrivateSNN* against these attacks, we synthesize the class representation of SNNs with and without encryption training. Fig. 6 shows 20 examples of generated image from CIFAR10 (top row) and TinyImageNet (bottom row). We visualize images from five configurations: original images, attack1 without encryption training, attack1 with encryption training, attack2 without encryption training, and attack2 with encryption training. We observe that SNNs without encryption training (*i.e.*, Fig. 6(b)) are vulnerable to attack1, showing important features of original classes. On the other hand, with temporal spike-based learning rule, attack1 does not discover any meaningful information as shown in Fig. 6(c). For attack2 (Fig. 6(d) and Fig. 6(e)), synthetic images show noisy results due to discrepancy between real gradients and approximated gradients. This comes from the intrinsic nature of SNNs, therefore SNNs are robust to attack2

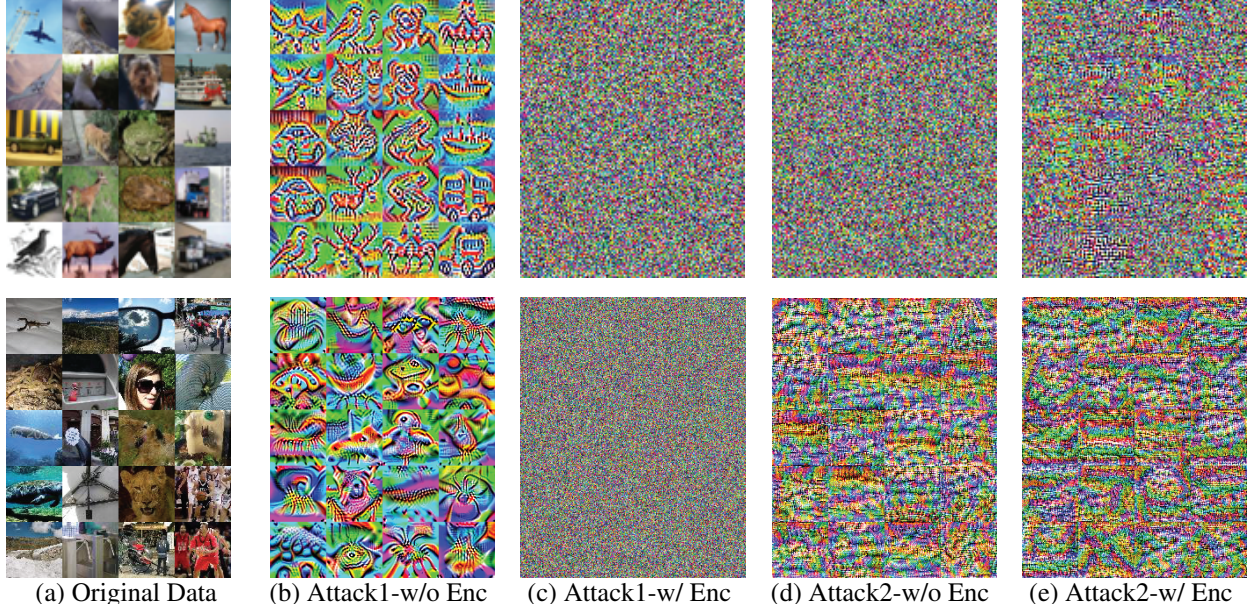


Figure 6. Qualitative results of two attack scenarios on the class leakage problem (top row: CIFAR10 / bottom row: TinyImageNet). “Enc” denotes encryption training with spike-based learning rule.

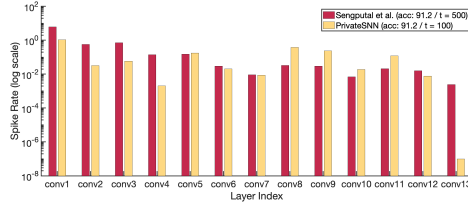


Figure 7. Spike rate (log scale) across all layers in VGG16 trained on CIFAR10.

Table 4. Energy efficiency comparison with VGG16 on CIFAR10.

Method	#Time-step	Acc (%)	E_{ANN}/E_{method}
VGG16 (ANN) [46]	1	91.5	1 \times
Sengupta et al. [44]	500	91.2	27.9 \times
PrivateSNN (ours)	100	91.2	59.3 \times

even without encryption. Overall, *PrivateSNN* is an effective solution to class leakage problem.

We quantify the security of the model by measuring how much generated images represent similar features with that of original images. To this end, we use *Fréchet inception distance* (FID) metric [20] that is widely used in GAN evaluation [36, 35]. The FID score compares the statistics of embedded features in a feature space of the pre-trained Inception V3 model. Thus, a lower FID score means that the generated images provide the original data-like feature. In Table 3, the SNN model without encryption training on attack scenario 1 achieves a much lower FID score (*i.e.*, 354.8) compared to the others, which supports our visualization results.

5.5. Energy-efficient PrivateSNN

In addition to privacy, SNNs are well known for high energy-efficiency compared to ANN. Therefore, we com-

pute the energy consumption of ANNs and SNNs. We calculate the energy based on the spike rate (*i.e.*, the average number of spikes across time) of all layers. In Fig. 7, we visualize the spike rate of Sengupta *et al.* [44] and *PrivateSNN*. We observe that *PrivateSNN* shows fewer spikes activity since we use a small number of time-steps. This lead to a huge energy-efficiency on standard CMOS technology [22]. As shown in Table 4, *PrivateSNN* shows 59.3 \times higher energy efficiency compared to standard ANN. Thus, *PrivateSNN* not only brings privacy but also energy-efficiency to the neuromorphic system. It is worth mentioning that SNNs can obtain much higher energy-efficiency on neuromorphic hardware platform [1, 11].

6. Conclusion

In this work, we propose *PrivateSNN* which successfully converts ANNs to SNNs without exposing sensitive information. Our main contributions can be summarized as follows:

- For the first time, we tackle the privacy issue around data and class leakage with SNN conversion.
- We encrypt the weight parameters of SNNs with temporal information, which makes networks difficult to be interpreted in the spatial domain.
- Knowledge distillation from the ANN model to SNNs enables stable encryption training with fewer training samples.
- *PrivateSNN* successfully hides sensitive information and also achieves huge energy-efficiency compared to standard ANN.

7. Acknowledgement

The research was funded in part by C-BRIC, one of six centers in JUMP, a Semiconductor Research Corporation (SRC) program sponsored by DARPA, the National Science Foundation (Grant#1947826), and the Amazon Research Award.

References

- [1] Filipp Akopyan, Jun Sawada, Andrew Cassidy, Rodrigo Alvarez-Icaza, John Arthur, Paul Merolla, Nabil Imam, Yutaka Nakamura, Pallab Datta, Gi-Joon Nam, et al. Truenorth: Design and tool flow of a 65 mw 1 million neuron programmable neurosynaptic chip. *IEEE transactions on computer-aided design of integrated circuits and systems*, 34(10):1537–1557, 2015.
- [2] Guo-qiang Bi and Mu-ming Poo. Synaptic modifications in cultured hippocampal neurons: dependence on spike timing, synaptic strength, and postsynaptic cell type. *Journal of neuroscience*, 18(24):10464–10472, 1998.
- [3] Tim VP Bliss and Graham L Collingridge. A synaptic model of memory: long-term potentiation in the hippocampus. *Nature*, 361(6407):31–39, 1993.
- [4] Mike Davies, Narayan Srinivasa, Tsung-Han Lin, Gautham Chinya, Yongqiang Cao, Sri Harsha Choday, Georgios Dimou, Prasad Joshi, Nabil Imam, Shweta Jain, et al. Loihi: A neuromorphic manycore processor with on-chip learning. *IEEE Micro*, 38(1):82–99, 2018.
- [5] Jia Deng, Wei Dong, Richard Socher, Li-Jia Li, Kai Li, and Li Fei-Fei. Imagenet: A large-scale hierarchical image database. In *2009 IEEE conference on computer vision and pattern recognition*, pages 248–255. Ieee, 2009.
- [6] Peter U Diehl and Matthew Cook. Unsupervised learning of digit recognition using spike-timing-dependent plasticity. *Frontiers in computational neuroscience*, 9:99, 2015.
- [7] Peter U Diehl, Daniel Neil, Jonathan Binas, Matthew Cook, Shih-Chii Liu, and Michael Pfeiffer. Fast-classifying, high-accuracy spiking deep networks through weight and threshold balancing. In *2015 International Joint Conference on Neural Networks (IJCNN)*, pages 1–8. ieee, 2015.
- [8] Yan Fang, Zheng Wang, Jorge Gomez, Suman Datta, Asif I Khan, and Arijit Raychowdhury. A swarm optimization solver based on ferroelectric spiking neural networks. *Frontiers in neuroscience*, 13:855, 2019.
- [9] E Paxon Frady, Garrick Orchard, David Florey, Nabil Imam, Ruokun Liu, Joyesh Mishra, Jonathan Tse, Andreas Wild, Friedrich T Sommer, and Mike Davies. Neuromorphic nearest neighbor search using intel’s pohoiki springs. In *Proceedings of the Neuro-inspired Computational Elements Workshop*, pages 1–10, 2020.
- [10] Matt Fredrikson, Somesh Jha, and Thomas Ristenpart. Model inversion attacks that exploit confidence information and basic countermeasures. In *Proceedings of the 22nd ACM SIGSAC Conference on Computer and Communications Security*, pages 1322–1333, 2015.
- [11] Steve B Furber, Francesco Galluppi, Steve Temple, and Luis A Plana. The spinnaker project. *Proceedings of the IEEE*, 102(5):652–665, 2014.
- [12] Ross Girshick. Fast r-cnn. In *Proceedings of the IEEE international conference on computer vision*, pages 1440–1448, 2015.
- [13] Ian Goodfellow, Jean Pouget-Abadie, Mehdi Mirza, Bing Xu, David Warde-Farley, Sherjil Ozair, Aaron Courville, and Yoshua Bengio. Generative adversarial nets. In *Advances in neural information processing systems*, pages 2672–2680, 2014.
- [14] Ian J Goodfellow, Jonathon Shlens, and Christian Szegedy. Explaining and harnessing adversarial examples. *arXiv preprint arXiv:1412.6572*, 2014.
- [15] Bing Han and Kaushik Roy. Deep spiking neural network: Energy efficiency through time based coding. In *Proc. IEEE Eur. Conf. Comput. Vis. (ECCV)*, pages 388–404, 2020.
- [16] Bing Han, Gopalakrishnan Srinivasan, and Kaushik Roy. Rmp-snn: Residual membrane potential neuron for enabling deeper high-accuracy and low-latency spiking neural network. In *Proceedings of the IEEE/CVF Conference on Computer Vision and Pattern Recognition*, pages 13558–13567, 2020.
- [17] Matan Haroush, Itay Hubara, Elad Hoffer, and Daniel Soudry. The knowledge within: Methods for data-free model compression. In *Proceedings of the IEEE/CVF Conference on Computer Vision and Pattern Recognition*, pages 8494–8502, 2020.
- [18] Kaiming He, Xiangyu Zhang, Shaoqing Ren, and Jian Sun. Deep residual learning for image recognition. pages 770–778, 2016.
- [19] Donald Olding Hebb. *The organization of behavior: A neuropsychological theory*. Psychology Press, 2005.
- [20] Martin Heusel, Hubert Ramsauer, Thomas Unterthiner, Bernhard Nessler, and Sepp Hochreiter. Gans trained by a two time-scale update rule converge to a local nash equilibrium. *arXiv preprint arXiv:1706.08500*, 2017.
- [21] Geoffrey Hinton, Oriol Vinyals, and Jeff Dean. Distilling the knowledge in a neural network. *arXiv preprint arXiv:1503.02531*, 2015.
- [22] Mark Horowitz. 1.1 computing’s energy problem (and what we can do about it). In *2014 IEEE International Solid-State Circuits Conference Digest of Technical Papers (ISSCC)*, pages 10–14. IEEE, 2014.
- [23] Sergey Ioffe and Christian Szegedy. Batch normalization: Accelerating deep network training by reducing internal covariate shift. *arXiv preprint arXiv:1502.03167*, 2015.
- [24] Seijoon Kim, Seongsik Park, Byunggook Na, and Sungroh Yoon. Spiking-yolo: Spiking neural network for real-time object detection. *arXiv preprint arXiv:1903.06530*, 1, 2019.
- [25] Youngeun Kim, Donghyeon Cho, and Sungeun Hong. Towards privacy-preserving domain adaptation. *IEEE Signal Processing Letters*, 27:1675–1679, 2020.
- [26] Youngeun Kim and Priyadarshini Panda. Revisiting batch normalization for training low-latency deep spiking neural networks from scratch. *arXiv preprint arXiv:2010.01729*, 2020.

[27] Youngeun Kim and Priyadarshini Panda. Visual explanations from spiking neural networks using interspike intervals. *arXiv preprint arXiv:2103.14441*, 2021.

[28] Alex Krizhevsky, Geoffrey Hinton, et al. Learning multiple layers of features from tiny images. 2009.

[29] Jogendra Nath Kundu, Naveen Venkat, R Venkatesh Babu, et al. Universal source-free domain adaptation. In *Proceedings of the IEEE/CVF Conference on Computer Vision and Pattern Recognition*, pages 4544–4553, 2020.

[30] Chankyu Lee, Syed Shakib Sarwar, Priyadarshini Panda, Gopalakrishnan Srinivasan, and Kaushik Roy. Enabling spike-based backpropagation for training deep neural network architectures. *Frontiers in Neuroscience*, 14, 2020.

[31] Jun Haeng Lee, Tobi Delbrück, and Michael Pfeiffer. Training deep spiking neural networks using backpropagation. *Frontiers in neuroscience*, 10:508, 2016.

[32] Xianfeng Li, Weijie Chen, Di Xie, Shicai Yang, Peng Yuan, Shiliang Pu, and Yueling Zhuang. A free lunch for unsupervised domain adaptive object detection without source data. *arXiv preprint arXiv:2012.05400*, 2020.

[33] Zhizhong Li and Derek Hoiem. Learning without forgetting. *IEEE transactions on pattern analysis and machine intelligence*, 40(12):2935–2947, 2017.

[34] Jian Liang, Dapeng Hu, and Jiashi Feng. Do we really need to access the source data? source hypothesis transfer for unsupervised domain adaptation. In *International Conference on Machine Learning*, pages 6028–6039. PMLR, 2020.

[35] Takeru Miyato, Toshiki Kataoka, Masanori Koyama, and Yuichi Yoshida. Spectral normalization for generative adversarial networks. *arXiv preprint arXiv:1802.05957*, 2018.

[36] Takeru Miyato and Masanori Koyama. cegans with projection discriminator. *arXiv preprint arXiv:1802.05637*, 2018.

[37] Konda Reddy Mopuri, Phani Krishna Uppala, and R Venkatesh Babu. Ask, acquire, and attack: Data-free user generation using class impressions. In *Proceedings of the European Conference on Computer Vision (ECCV)*, pages 19–34, 2018.

[38] Gaurav Kumar Nayak, Konda Reddy Mopuri, Vaisakh Shah, Venkatesh Babu Radhakrishnan, and Anirban Chakraborty. Zero-shot knowledge distillation in deep networks. In *International Conference on Machine Learning*, pages 4743–4751. PMLR, 2019.

[39] Emre O Neftci, Hesham Mostafa, and Friedemann Zenke. Surrogate gradient learning in spiking neural networks. *IEEE Signal Processing Magazine*, 36:61–63, 2019.

[40] Adam Paszke, Sam Gross, Soumith Chintala, Gregory Chanan, Edward Yang, Zachary DeVito, Zeming Lin, Alban Desmaison, Luca Antiga, and Adam Lerer. Automatic differentiation in pytorch. In *NIPS-W*, 2017.

[41] Nitin Rathi, Gopalakrishnan Srinivasan, Priyadarshini Panda, and Kaushik Roy. Enabling deep spiking neural networks with hybrid conversion and spike timing dependent backpropagation. *arXiv preprint arXiv:2005.01807*, 2020.

[42] Kaushik Roy, Akhilesh Jaiswal, and Priyadarshini Panda. Towards spike-based machine intelligence with neuromorphic computing. *Nature*, 575(7784):607–617, 2019.

[43] Bodo Rueckauer, Iulia-Alexandra Lungu, Yuhuang Hu, Michael Pfeiffer, and Shih-Chii Liu. Conversion of continuous-valued deep networks to efficient event-driven networks for image classification. *Frontiers in neuroscience*, 11:682, 2017.

[44] Abhroni Sengupta, Yuting Ye, Robert Wang, Chiao Liu, and Kaushik Roy. Going deeper in spiking neural networks: Vgg and residual architectures. *Frontiers in neuroscience*, 13:95, 2019.

[45] Saima Sharmin, Nitin Rathi, Priyadarshini Panda, and Kaushik Roy. Inherent adversarial robustness of deep spiking neural networks: Effects of discrete input encoding and non-linear activations. *arXiv preprint arXiv:2003.10399*, 2020.

[46] Karen Simonyan and Andrew Zisserman. Very deep convolutional networks for large-scale image recognition. 2015.

[47] Nitish Srivastava, Geoffrey Hinton, Alex Krizhevsky, Ilya Sutskever, and Ruslan Salakhutdinov. Dropout: a simple way to prevent neural networks from overfitting. *The journal of machine learning research*, 15(1):1929–1958, 2014.

[48] Yujie Wu, Lei Deng, Guoqi Li, Jun Zhu, and Luping Shi. Spatio-temporal backpropagation for training high-performance spiking neural networks. *Frontiers in neuroscience*, 12:331, 2018.

[49] Qi Xu, Jianxin Peng, Jiangrong Shen, Huajin Tang, and Gang Pan. Deep covdensesnn: A hierarchical event-driven dynamic framework with spiking neurons in noisy environment. *Neural Networks*, 121:512–519, 2020.

[50] Jason Yosinski, Jeff Clune, Anh Nguyen, Thomas Fuchs, and Hod Lipson. Understanding neural networks through deep visualization. *arXiv preprint arXiv:1506.06579*, 2015.

[51] Li Yuan, Francis EH Tay, Guilin Li, Tao Wang, and Jiashi Feng. Revisit knowledge distillation: a teacher-free framework. *arXiv preprint arXiv:1909.11723*, 2019.

[52] Yuheng Zhang, Ruoxi Jia, Hengzhi Pei, Wenxiao Wang, Bo Li, and Dawn Song. The secret revealer: Generative model-inversion attacks against deep neural networks. In *Proceedings of the IEEE/CVF Conference on Computer Vision and Pattern Recognition*, pages 253–261, 2020.

[53] Bo Zhao, Konda Reddy Mopuri, and Hakan Bilen. idlg: Improved deep leakage from gradients. *arXiv preprint arXiv:2001.02610*, 2020.

[54] Ligeng Zhu and Song Han. Deep leakage from gradients. In *Federated Learning*, pages 17–31. Springer, 2020.